

Low-frequency fluctuations in semiconductor ring lasers with optical feedback

Lilia Mashal¹, Romain Modeste Nguimdo¹, Guy Van der Sande¹, Miguel C. Soriano², Jan Danckaert¹, and Guy Verschaffelt¹

Abstract—In this paper, we experimentally and numerically study the dynamics of semiconductor ring lasers subjected to long delay and moderate self-feedback. By varying the pump current and/or the feedback strength, we study the appearance and the parameter dependence of low frequency fluctuations in these systems. In particular, we observe different routes to the building up of the initial power amplitude.

Index Terms—Semiconductor ring lasers, low-frequency fluctuations, nonlinear dynamics

I. INTRODUCTION

SEMICONDUCTOR lasers subject to external feedback are known to exhibit a wide variety of dynamical regimes desired for some applications such as chaos cryptography [1]–[3], random bit generation [4], [5] and reservoir computing [6]. Out of those, chaotic intensity fluctuations, coherence collapse (CC) [7], [8] and low-frequency fluctuations (LFF) [9], [10] are the most frequently encountered behaviors. The latter is characterized by a fast drop of the laser intensity [11], [12] followed by a gradual recovery process. The duration of this recovery process is irregular and is of the order of hundred of nanoseconds. The average time between the dropouts is much larger than the laser system characteristic time-scales (the relaxation oscillation and the external cavity round-trip time). Typically LFFs are unwanted because they may disrupt the proper working of the device. Thus several works have been devoted to this phenomenon, mainly to understand in which conditions it emerges in order to efficiently avoid it [9], [13].

The physical interpretation of the LFF regime was under a strong debate for over a decade. Mork *et al.* suggested that the LFFs arise due to the bistability of the external cavity modes, i.e. bistability between the maximum gain mode and a lower intensity state [10], [14]. Sacher *et al.* demonstrated that the LFFs take place on a chaotic attractor [15]. Importantly, the main origin of the dropouts for a single-mode semiconductor laser was first described by Sano *et al.* [16] in the context of the Lang-Kobayashi equations [17]. According to this interpretation, the LFF regime is shown to be a deterministic chaotic itinerancy process towards the external cavity mode with the largest gain, in which the dropout is caused by the crises between the antimodes and the local

chaotic attractor [16]. Even though this model is sufficient to reproduce the LFF process, the precise laser operations observed experimentally may sometimes require an extended model with the inclusion of additional longitudinal modes and spontaneous emission noise. In particular, it has been shown that spontaneous-emission can induce dropouts in the laser output [18], [19]. So far, the LFF regime has been observed in different types of semiconductor lasers, e.g. in edge-emitting lasers [9], [10], [12], [14], [20], [21], VCSELs [22], [23] and multimode semiconductor diode lasers with frequency selective feedback [24]. For some lasers, it has been found that LFFs can even coexist with other regimes such as stable oscillations [25], [26]. For the exact dynamical operation within the LFF regime, it is known that the feedback strength, the pump current and the external cavity length play an important role in the emergence of LFFs [26]. At this point, we note that LFFs typically appear close to the threshold current of the laser, but can also emerge well above threshold. By way of illustration, in Ref. [27] sporadic power discontinuities manifesting through power spikes above the threshold have been observed far away from the threshold. For an increasing pump current, the LFF regime evolves into the fully developed coherence collapse regime.

Semiconductor ring lasers (SRLs) are currently the focus of a rapidly thriving research activity due to their unique feature of directional bistability [28], [29], which opens up the possibility of using them in systems for all-optical switching, gating, wavelength-conversion functions, and optical memories [30]–[35]. SRLs do not require cleaved facets or gratings for optical feedback and are thus particularly suited for a monolithic integration [36]. Moreover, SRLs have been recognized to be ideal optical prototypes of nonlinear Z2-symmetric systems [37] exhibiting in the solitary case, multistable [38] and excitable behavior [39]. When SRLs are perturbed by optical injection from another laser, the symmetry of their phase space leads to a novel route to chaos [40]. In the case of SRLs with delayed optical feedback, it has been shown that their ability to lase simultaneously in two directional modes facilitates the generation of chaotic signals with time-delay concealment both in the intensity and the phase [41], the generation of square wave oscillations [42] or random bits generation using bitwise Exclusive-OR operations [43]. Thus from a fundamental perspective, it is of great interest to investigate under which conditions, dynamical regimes, such as LFF, may occur in order to control chaotic behavior by laser parameter tuning. In this paper we experimentally and numerically address this issue considering a SRL in a feedback

¹ Applied Physics Research Group (APHY), Vrije Universiteit Brussel, Pleinlaan 2, 1050 Brussel, Belgium e-mail: lmashal@vub.ac.be

²Instituto de Física Interdisciplinar y Sistemas Complejos, IFISC (CSIC-UIB), Campus Universitat de les Illes Balears, E-07122 Palma de Mallorca, Spain

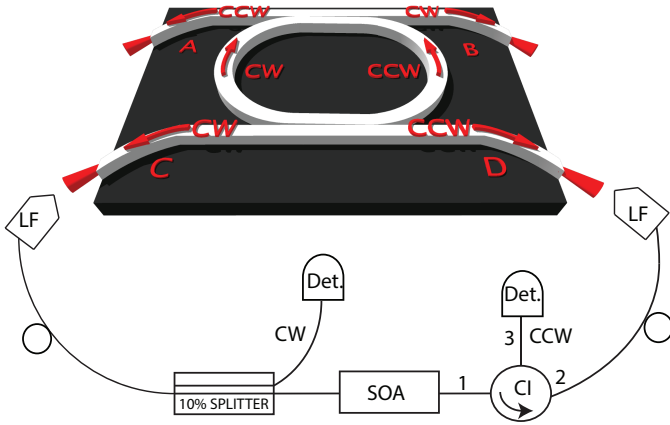


Fig. 1: A schematic setup of the semiconductor ring laser subject to optical feedback. LF is the lensed fiber, SOA the semiconductor optical amplifier and CI the circulator.

configuration where only one directional mode is re-injected into the same directional mode. The results show that the LFF power drop-outs can be observed for a large range of parameters including those for which the laser operates far above the lasing threshold. We also find the coexistence of two recovery processes, i.e. stepwise recovery and recovery accompanied by a train of pulses.

The paper is structured as follows. In Section 2 we describe the experimental setup. The qualitatively different dynamical regimes that can be observed in the device are presented in Section 3. We give an overview of the dynamics of this phenomenon and characterize the power drop-outs by presenting experimental time series. We analyze the recovery process for the power dropouts in detail. In Section 4 we present numerical modeling of LFF in SRLs based on rate-equations with delayed optical feedback. Finally, a summary and conclusions are given in Section 5.

II. EXPERIMENTAL SETUP

The experiments are performed on an AlGaInAs/InP-based multi-quantum-well semiconductor ring laser (SRL) with a racetrack geometry that has been fabricated at Glasgow University. The racetrack-shaped ring cavity has two semicircular sections with $200 \mu\text{m}$ radius and two $75 \mu\text{m}$ straight sections. The cavity's free-spectral-range is measured to be 53.6 GHz . The device is a monolithically integrated four-port SRL, where two access waveguides are coupled to the ring cavity by forming directional couplers with the straight sections, providing about 30% coupling ratio. The access waveguides form a 10° angle with the cleaved bar facets to minimize back-reflection. The SRL operates in a single-transverse, single-longitudinal mode at $\lambda = 1560 \text{ nm}$ when no feedback is applied. A schematic representation of the measurement setup with such a SRL is shown in Fig. 1. The geometry of the ring cavity supports two directional modes: a clockwise (CW) and a counterclockwise (CCW) propagating mode. Directional couplers allow to couple out parts of the light from the ring in the output waveguides. As shown in Fig. 1, there are four

ports (A, B, C, and D) at the facets of the chip that serve as SRL inputs or outputs. Lensed optical fibers can be aligned to these ports. The device is mounted on a copper chuck and thermally controlled by a Peltier element to the temperature T_{chip} with an accuracy of 0.01°C . In Fig. 2 we plot the optical power measured in the CW and CCW directions as a function of the SRL pumping current when no feedback is applied. The SRL has a threshold current of 47 mA . Above and close to the threshold, the SRL resides in the bidirectional regime where it emits both directional modes up to about 75 mA . Above 75 mA , one mode takes over the other and therefore, the laser emits a unidirectional mode.

The feedback loop is implemented using lensed fibers connected to ports C and D. The round trip time of the external cavity is given by $\tau = nL/c$, where L is the length of the external cavity, c is the speed of light and $n = 1.5$ is the refractive index for the optical fibers used in the feedback loop. Here L is 12 m , yielding the delay time $\tau \approx 60 \text{ ns}$. A semiconductor optical amplifier (SOA) is placed in the feedback loop to control the feedback strength by changing the current in the SOA. In all of the experiments, the saturation power of the SOA (model Thorlabs SOA1117S) is larger than the input signal from the SRL that is amplified, such that the SOA is always operated in its linear gain regime. The SOA gain depends on its pump current. For a SOA current of 0 mA , the SOA is strongly absorbing. For SOA currents between 200 mA and 600 mA , the SOA gain increases approximately linearly from 7.5 dB to 20 dB . Above 600 mA the gain of the SOA starts to saturate. The SOA will also generate amplified spontaneous emission (ASE) noise that is injected in both directions. The ASE power is $34 \mu\text{W}$ at 200 mA and increases to 1.3 mW at a SOA current of 600 mA . This is much higher than the power emitted from the SRL, but this ASE power is emitted at all wavelengths ranging from 1520 nm to 1580 nm . Therefore, only a small amount of the ASE power is injected in the SRL's lasing mode, which we neglect in our analysis. The fiber-based splitter is used in the setup to read out the CW mode by detecting it with a fast photodiode with bandwidth of 2.4 GHz connected to a real-time oscilloscope with bandwidth of 4 GHz . The fiber coupled output of the SOA is connected to port 1 of a circulator. The circulator transmits light from port 1 to port 2, which in its turn is connected to port D of the SRL chip via a lensed optical fiber. Hence the CW directional mode of the SRL taken from port C of the chip is re-injected in port D, i.e. in CW direction (single self-feedback). On the contrary, the CCW mode coupled out from port D, is removed from the feedback loop by the circulator (ports 2-3) and used for characterization purposes. Light from port 3 of the circulator is detected by a fast photodiode connected to an oscilloscope. In order to avoid optical feedback from the facets of the chip the output waveguides are tilted by 10° with respect to the chip facets. Therefore, to increase the output power and couple the light of the chip efficiently, the fibers are angled at 32° with respect to the facet's normal. Moreover, an independent bias current I_{WG} on the output waveguide of port D is provided in order to amplify the light traveling through this waveguide.

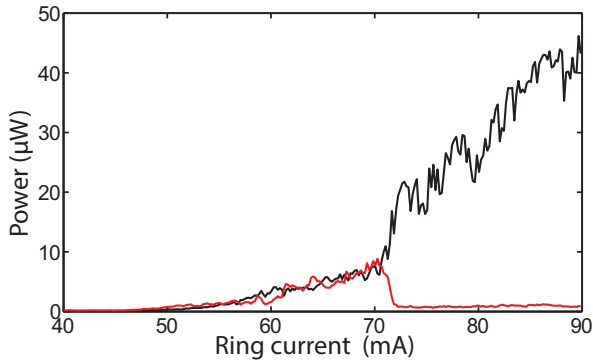


Fig. 2: SRLs optical output power in CW (red) and CCW (black) directions. $I_{WG}=14$ mA, and mount temperature is 23°C .

III. EXPERIMENTAL RESULTS

To begin with, we set the SRL injection current to 92 mA and the current on the SOA to 700 mA. We simultaneously detect the CW and CCW directional mode outputs using AC-photodiodes with a bandwidth of 2.4 GHz. Figure 3 (a) shows the dynamical evolution of the system for both modes. This figure shows the typical slow drop-out and recovery behavior of LFF. The dynamics of semiconductor lasers with delayed feedback is characterized by high frequency pulsations in the picoseconds range. In fact the majority of the energy will be concentrated in the high frequency components of the system. In our experiments [such as in Figure 3(a)], we cannot observe these pulses due to the limited bandwidth of the measuring equipment. Nevertheless, this cut-off frequency at 2.4 GHz already allows to identify the slow time LFF phenomenon but with still some significant high-frequency oscillations superimposed. The bandwidth corresponding to the LFF behavior was determined from RF spectra showing an increase below 5 MHz corresponding to this slow timescale dynamics. In this paper, it is our intention to characterize only the low frequency events in detail. Also, a large contribution to the signal at higher frequencies is due to the noise of the oscilloscope and detector, which we want to remove. For these reasons, we have decided to filter out the high frequency part of the signal. The used filter is a second order low-pass Butterworth filter with a bandwidth of 125 MHz. This bandwidth is high enough, such that the LFFs slow time scale fluctuations are not strongly influenced by the filter.

Since the feedback is implemented in only one directional mode, the CW mode shows typical LFF dynamics characterized by power dropouts. The intensity does not drop to zero during the so-called dropout events. Even if we remove the 125 MHz bandwidth filter, the drop out does not reach the zero level because of the 2.4GHz bandwidth of the detector. Interestingly, we also observe power spikes in the CCW mode. As can be seen, the power fluctuations in the CW and CCW modes are anti-correlated, i.e. a dropout in the CW direction coincides with a spike in the CCW direction. This out-of-phase dynamics originates from the coupling between the directional modes via the carrier reservoir, which is shared

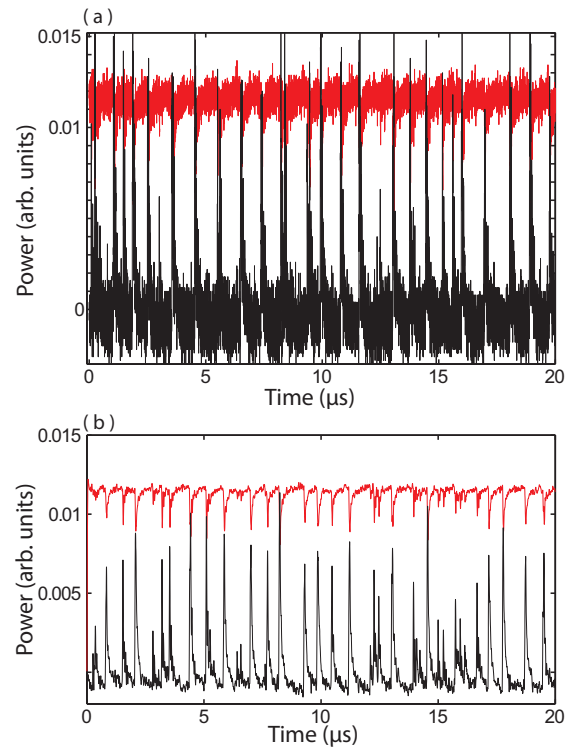


Fig. 3: (a) Time traces of the intensity of the CW mode (red), and the CCW mode (black). (b) Time traces of the intensities after filtering with a low-pass filter (with a bandwidth of 125 MHz). The SRL injection current is 92 mA and the current in the SOA is $I_{SOA} = 700$ mA.

by the two directional modes as in VCSELs [23]. The time between consecutive dropouts is not a constant, and varies between $0.6 \mu\text{s}$ and $1.4 \mu\text{s}$, corresponding to 10-20 times the delay time τ .

In the literature, the LFF recovery process has been often denoted as stepwise (see e.g. Ref. [44]) and characterized by taking an average over several LFF events. Figure 4 shows an enlargement of Fig. 3 (b). In our experiment, two qualitatively different recovery processes can be distinguished after the laser intensity's sudden dropouts. In some instances, the build-up is done by a stepwise recovery. Here the average intensity is roughly locked to a certain level during each step. The time duration of each step in the power recovery is equal to the external cavity round-trip time. In other instances, the recovery is accompanied by a train of short pulses. The time between the pulses is equal to the external cavity round-trip time. The pulse amplitude decreases from pulse to pulse until the initial state is restored. The width of the pulses is on average 20 ns, but is not constant. The first pulse during the recovery has the largest amplitude and the smallest width. Subsequent pulses have a larger width while the amplitude lowers. We have noticed that the kind of recovery process is randomly varying from pulse to pulse. To the best of our knowledge, pulse and stepwise have not been distinguished as two distinct recovery processes. However, like LFFs not being specific to SRLs, we expect these recovery processes to appear also in VCSELs and edge-emitting lasers for similar feedback conditions as the

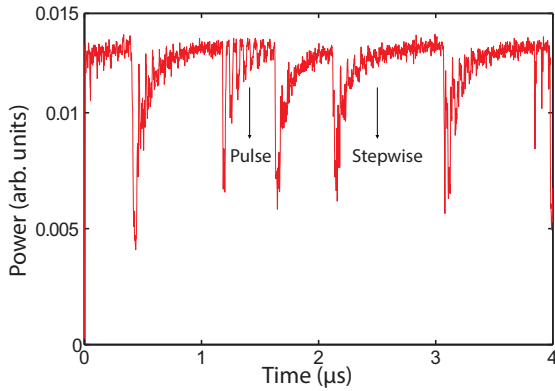


Fig. 4: Filtered time trace of the intensity of the CW mode depicting different LFF events at a SRL bias current of 92 mA and a SOA current of $I_{SOA} = 700$ mA.

ones studied here. Specifically, we expect these two different recovery processes to occur in feedback configurations with a rather long delay time. The physical mechanisms causing these recovery processes are not fully understood yet. Real-time spectroscopy techniques might help in elucidating their origin [45].

IV. PARAMETER DEPENDENCE

As already pointed out in the introduction, the LFF cycles depend on the pump current and the feedback strength. In our experiments, we first set the injection current constant at 90 mA. Then by varying the current in the SOA, we plot in Fig. 5 several time series of the CW directional mode. For $I_{SOA} = 0$ in Fig. 5(a), the laser resides in the uni-directional emission regime and most of the power is emitted in the CCW mode. Hence, the power in the CW mode is low.

By increasing I_{SOA} to 300 mA the laser shows a behavior characterized by alternate emission of constant and stable output in the CCW directional mode (low power in Fig. 5) and sudden random switches to the other directional mode [see Fig. 5 (b)]. This mode-hopping between the different dynamical regimes is irregular and seems to be noise driven as the residence time in each of the regimes follows an exponential distribution. When the SRL is emitting in the CCW mode, there is effectively no optical feedback and no feedback related dynamics is observed. However, after a mode-hopping event to the CW direction, the feedback loop is active and the output power is no longer stationary and short excursions to the CCW mode can be observed, some of which are reminiscent of a LFF cycle.

By further increasing I_{SOA} to 400 mA the system shows LFFs events [see Fig. 5 (c)]. We further increase the SOA current and observe that the dropout events become less frequent: the average time between LFF events ranges from $0.4 \mu\text{s}$ in Fig. 5 (c) to $1.0 \mu\text{s}$ in Fig. 5 (e).

To investigate the effect of the pump current, we keep the SOA current at 350 mA and plot, in Fig. 6, the time traces for various values of the pump current. We first set the injection current close to laser threshold and observe LFFs as in other lasers [9], [10], [12], [14], [20]–[23]. This regime

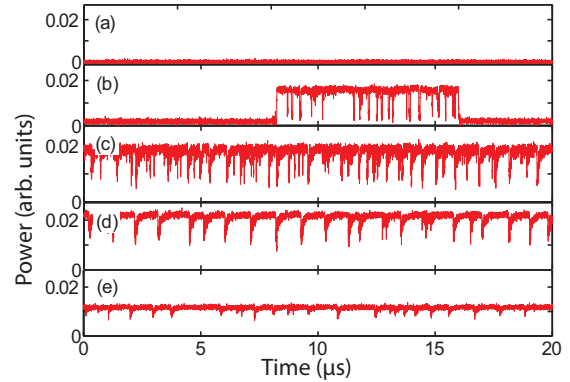


Fig. 5: Filtered time traces of the CW intensity for different SOA current. a) $I_{SOA} = 0$ mA, (b) $I_{SOA} = 300$ mA, (c) $I_{SOA} = 400$ mA, (d) $I_{SOA} = 500$ mA, (e) $I_{SOA} = 700$ mA. The SRL injection current is 90 mA.

is maintained as the injection current is increased far above the threshold. The average time between LFF events decreases with increasing injection current: it is $2.4 \mu\text{s}$ at an injection current of 58 mA and it decreases to $1.12 \mu\text{s}$ at an injection current of 90 mA, with $I_{SOA} = 350$ mA for both cases. The standard deviation does not change significantly when changing the injection current: it is $0.05 \mu\text{s}$ at an injection current of 58 mA and $0.042 \mu\text{s}$ at an injection current of 90 mA, [see the corresponding spikes of the CCW mode in Fig. 6 (a)-(d)]. The intensity spikes in the CCW direction also become larger for higher pumping current. Because the optical output power increases with injection current.

V. MODEL AND SIMULATIONS

In order to gain insight in the physical processes involved in the experimentally observed LFF, we perform numerical simulations considering a single longitudinal-mode SRL model [28], [38] extended with Lang-Kobayashi terms to account for the feedback [41], [46]. In terms of the mean electric fields

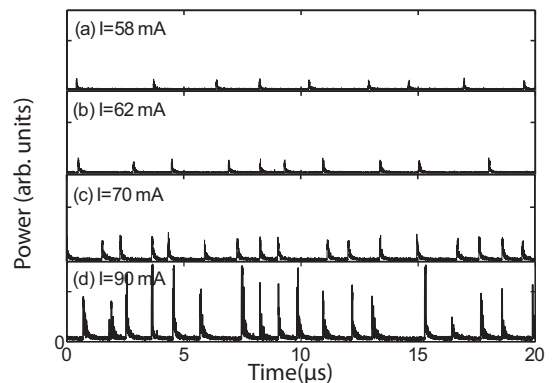


Fig. 6: Filtered time traces of the intensity of the CCW mode for different values of the SRL current I . The current on the output waveguide is $I_{WG} = 14$ mA, the mount temperature is 23°C and the current on the SOA is 350 mA.

E_{cw} and E_{ccw} of the counter propagating modes CW and CCW, respectively, and the carrier number inside the laser cavity N , the rate equations are

$$\dot{E}_{cw} = \kappa(1+i\alpha)[\mathcal{G}_{cw}N-1]E_{cw} - k(1-\delta_k)e^{i\phi_k}E_{ccw} + \eta E_{cw}(t-T)e^{-i\omega_0 T}, \quad (1)$$

$$\dot{E}_{ccw} = \kappa(1+i\alpha)[\mathcal{G}_{ccw}N-1]E_{ccw} - k(1+\delta_k)e^{i\phi_k}E_{cw}, \quad (2)$$

$$\dot{N} = \gamma \left[\mu - N - \mathcal{G}_{cw}N|E_{cw}|^2 - \mathcal{G}_{ccw}N|E_{ccw}|^2 \right], \quad (3)$$

where the parameters are the linewidth enhancement factor α , renormalized bias current μ , field decay rate κ , carrier inversion decay rate γ , solitary laser frequency ω_0 , feedback rate η , delay time T , feedback phase $\omega_0 T$, backscattering strength k and phase ϕ_k , respectively. A slight asymmetry in backscattering δ_k is considered, which accounts for e.g. reflections at the coupler being not perfectly the same for the CW and the CCW mode as motivated in Ref. [47]. The differential gain functions are given by $\mathcal{G}_{cw} = 1 - s|E_{cw}|^2 - c|E_{ccw}|^2$ and $\mathcal{G}_{ccw} = 1 - s|E_{ccw}|^2 - c|E_{cw}|^2$ where s and c account for the phenomenological self- and cross-saturations, respectively.

While parameters such as γ and κ are estimated from the cavity design and the quantum well material of the semiconductor ring lasers, the other parameters (α , the saturation coefficients and the backscattering parameters) are not measured. Nevertheless, together they determine the dynamical behaviour of the solitary semiconductor ring laser. Specifically, when raising the injection current from threshold on, the SRL first emits in a bi-directional mode, then goes in to an oscillatory regime and for higher currents it exhibits bistable uni-directional behaviour. The cascade of these regimes and the frequency of these oscillations is fixed by α , the saturation coefficients and the backscattering parameters. The relationship between the theoretical parameters and real-world devices are detailed in [28]. We consider: $\alpha = 3.5$, $\mu = 1.7$, $s = 0.005$, $c = 0.01$, $\kappa = 100 \text{ ns}^{-1}$, $\gamma = 0.2 \text{ ns}^{-1}$, $\omega_0 T = 0$, $k = 0.44 \text{ ns}^{-1}$, $\phi_k = 1.5$ and $T = 60 \text{ ns}$. μ and η are stated in the figure captions. An asymmetry in the backscattering will not be considered ($\delta k = 0$) unless stated otherwise. The time traces obtained by integrating Eqs. (1)-(3) are subsequently filtered using a low-pass fifth order butterworth filter with a bandwidth of 125 MHz.

Figure 7 (a) shows a part of the time traces of the power output from the CW (red) and CCW (black) directions, without filtering while Figure 7 (b) shows the corresponding filtered signals, considering $\mu = 3.0$ and $\eta = 40 \text{ ns}^{-1}$. Similar to the experimental observations shown in Fig. 3, the power dropout events in the CW mode and spikes events in the CCW mode alternate in a chaotic manner. We would like to point out that simulations are performed without addition of noise. In Fig. 8 we display an enlargement of the CW output signal considering different feedback strengths (left), as well as their corresponding trajectories projected onto the space of excess carrier number N and round trip phase difference, $\phi_{cw}(t) - \phi_{cw}(t-T)$ (right), all for a fixed pump current $\mu = 3.0$. We note that N , as well as $\phi_{cw}(t) - \phi_{cw}(t-T)$ have been filtered in the same manner as the intensities. In

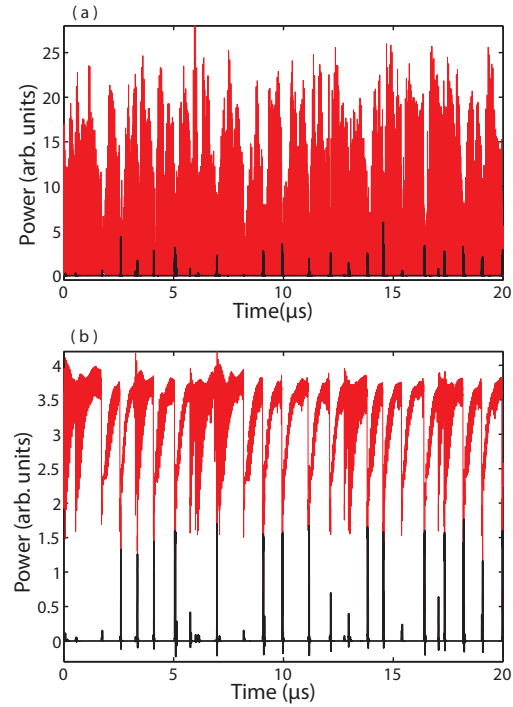


Fig. 7: (a) Intensity of CW mode (red), and CCW mode (black), (b) Filtered intensity of (a), obtained by numerical integration of Eqs. (1)-(3) with $\eta = 40 \text{ ns}^{-1}$ and $\mu = 3.0$.

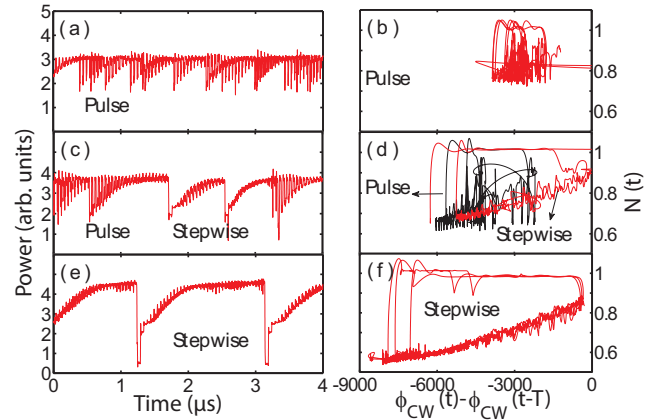


Fig. 8: Filtered intensity of the CW mode (left) and the corresponding trajectories in the phase space (right) obtained from by numerical integration for (a,b) $\eta = 30 \text{ ns}^{-1}$, (c,d) $\eta = 40 \text{ ns}^{-1}$ and (e,f) $\eta = 50 \text{ ns}^{-1}$ considering $\mu = 3.0$.

particular, the route to initial state recovery is seen when a power dropout event occurs. For $\eta = 30 \text{ ns}^{-1}$, the initial amplitude of the signal is recovered through a train of pulses [Fig. 8 (a)]. In this case, the phase space diagram looks closed [Fig. 8 (b)]. It is seen that during the power buildup process, the system exhibits a chaotic itinerancy between attractor ruins with a drift towards the maximum gain mode. When increasing to $\eta = 40 \text{ ns}^{-1}$, the dropout events in the CW mode become deeper and the initial state is recovered randomly either by a train of pulses as in Fig. 8 (a) or by steps [Fig. 8 (c)]. For further insight, we separately plot in Fig. 8 (d) the trajectories

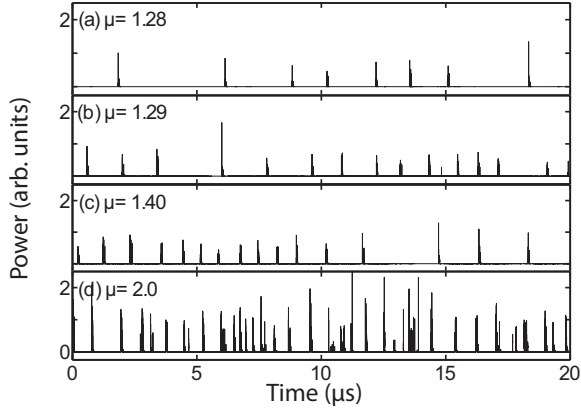


Fig. 9: Filtered intensity of the CCW mode obtained by numerical integration of Eqs. (1)-(3) with $\eta = 30\text{ns}^{-1}$, (a) $\mu = 1.28$ (b) $\mu = 1.29$, (c) $\mu = 1.4$, and (d) $\mu = 2.0$.

for the times between 0 and 1.5 μs (black) and between 1.5 μs and 3.0 μs (grey, red in color) which corresponds to pulses recovery and recovery accompanied by the train of stepwise in Fig. 8 (c), respectively. Further increasing η results in larger fluctuations in the modal intensity during the initial stage of a LFF cycle. We only observe a stepwise recovery in these cases. [Fig. 8 (e)]. This case shows a completely open diagram in phase space [Fig. 8 (f)]. In all the cases, the dynamics in the phase space do not repeat precisely from cycle to cycle due to the fact that the trajectories may visit different modes, and may collide with one of several nearby saddles. In fact, LFFs are a typical feature of the saddle node instability present in a nonlinear system. When the laser oscillates single mode or multimode, the fixed points fall into an ellipse composed by the so-called external cavity modes [16]. The dominant external cavity mode is the fixed point with the lowest carrier density or narrowest linewidth [48]. When the system is exhibiting LFF, the laser can hop to other existing points due to the unstable saddle node instability generated by the feedback [16]. Furthermore, Fig. 8 shows that by increasing the feedback strength the LFFs occur with a longer temporal separation.

In Fig. 9, we study the dependence of the dynamics on the pump current. We keep the feedback strength fixed to $\eta = 30\text{ns}^{-1}$, while varying the pump current in the range $\mu \in [1.28 - 2]$. For different values of the pump current, we find that as predicted from experimental results (see Figure 6) by increasing the pumping current, dropouts or spikes become more frequent.

Finally, we will try to capture the noise induced hopping between the CCW and CW mode as observed experimentally in Fig. 5(b). We add to Eq. (1) and (2) white noise terms \tilde{F}_{cw} and \tilde{F}_{ccw} , respectively, described by the correlations $\langle \tilde{F}_i(t')\tilde{F}_j(t) \rangle = 2\beta N\delta_{ij}\delta(t-t')$, where $i, j \in \{cw, ccw\}$ and β is the noise strength. To observe the hopping, a careful balance is required between a slight asymmetry in the backscattering and a rather low feedback strength. We fix the backscattering asymmetry $\delta k = 0.2$. In this case, for zero

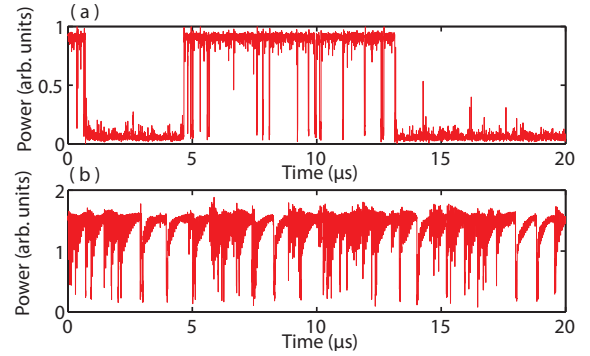


Fig. 10: Filtered intensity of the CW mode obtained by numerical integration of Eqs. (1)-(3) with $\mu=2.0$, $\delta_k=0.2$ and $\beta = 10^{-3}\text{ns}^{-1}$ (a) $\eta = 0.2\text{ns}^{-1}$ (b) $\eta = 25\text{ns}^{-1}$.

feedback strength, the SRL will have a strong preference to lase in the CCW mode as also observed experimentally in Fig. 5(a). The optical feedback (which is only in the CW mode) can cancel this preference, ensuring that it is equally likely to lase in one or the other mode. In fact, depending on the backscatter strength k , its phase ϕ_k and its asymmetry δ_k , the feedback strength η and its phase $\omega_0 T$, several bistable and multistable scenarios can be found. The study of these scenarios lies outside of the scope of this paper. In Fig. 10(a), it is clear that in this case the SRL can hop between the CCW mode (low power) and the CW mode (high power). A solitary SRL with a slightly broken symmetry in the backscattering is known to exhibit noise induced excitability (see e.g. Ref. [39]). Here, with feedback, these short noisy excursions can also be observed when the SRL is lasing in the CW mode [in Fig. 10(a)]. Interestingly, while emitting in the CCW mode and effectively experiencing no feedback, the SRL exhibits no excitable excursions to the other mode. As such the excitability is induced by the optical feedback. As the noise itself can alter the feedback dynamics, we have added numerical results for stronger feedback levels where the LFF are already developing [see Fig. 10(b)]. These numerical results clearly resemble the experimental results of Fig. 5(c). We would like to note that the backscattering and any backscattering asymmetry will only play a significant role in the dynamical behaviour of SRLs with delayed feedback at low feedback levels.

VI. CONCLUSION

In this paper we have presented experimental and numerical investigations of the dynamical behavior of a semiconductor ring lasers subject to self-optical feedback. In particular, we have investigated the appearance and the parameter dependence of LFFs in these SRLs with a preferential propagation direction of the feedback light. We observed that the system is very sensitive to feedback strength and the injection current. In particular, the power dropouts become less frequent when the feedback strength is increased or the pump current is decreased. In addition, we find two different recovery processes after the LFF power dropouts. The recovery can either occur via pulses or in a stepwise manner. Since LFFs are not specific to SRL, we expect these recovery processes to appear also

in VCSELs and edge-emitting lasers under similar feedback conditions as the ones studied here. The numerical simulations also capture these different behaviors, where the representation in the phase space of the carriers versus the round trip phase difference gives additional insight into these phenomena.

ACKNOWLEDGEMENTS

This research was supported by the Interuniversity Attraction Poles program of the Belgian Science Policy Office, under grant IAP P7-35 "Photonics@be", by the European project PHOCUS (EU FET-Open grant: 240763) and by the Hercules Foundation under the project "High-speed real-time characterization of photonic components". We acknowledge the Research Foundation-Flanders (FWO) for individual support and project funding. Furthermore, we thank Gabor Mezosi and Marc Sorel for the fabrication of the semiconductor ring lasers on which the experiments have been performed. The technical team of the James Watt Nanofabrication Centre is also gratefully acknowledged for the support in fabricating the devices.

REFERENCES

- [1] S. Donati and C.R. Mirasso, "Introduction to the feature section on optical chaos and applications to cryptography," *IEEE J. Quantum Electron.*, vol. 38, n. 9, pp. 1138–1140, 2002.
- [2] A. Argyris, D. Syvridis, L. Larger, V. Annovazzi-Lodi, P. Colet, I. Fischer, J. Garcia-Ojalvo, C.R. Mirasso, L. Pesquera, K.A. Shore, "Chaos-based communications at high bit rates using commercial fibre-optic links," *Nature*, vol. 438, n. 7066, pp. 343–346, 2005.
- [3] M. C. Soriano, P. Colet, and C. R. Mirasso, "Security implications of open-and closed-loop receivers in all-optical chaos-based communications," *IEEE Photon. Technol. Lett.*, vol. 21, n. 7, pp. 426–428, 2009.
- [4] A. Uchida, K. Amano, M. Inoue, K. Hirano, S. Naito, H. Someya, I. Oowada, T. Kurashige, M. Shiki, S. Yoshimori, K. Yoshimura, and P. Davis, "Fast physical random bit generation with chaotic semiconductor lasers," *Nat. Photonics*, vol. 2, n. 12, pp. 728–732, 2008.
- [5] T. E. Murphy, and R. Roy, "Chaotic lasers: The world's fastest dice," *Nat. Photonics*, vol. 2, n. 12, pp. 714–715, 2008.
- [6] L. Appeltant, M. C. Soriano, G. Van der Sande, J. Danckaert, S. Massar, J. Dambre, B. Schrauwen, C. R. Mirasso, and I. Fischer, "Information processing using a single dynamical node as complex system," *Nat. Commun.* vol. 2, 468, 2011.
- [7] J. S. Cohen and D. Lenstra, "The critical amount of optical feedback: for coherence collapse in semiconductor lasers," *IEEE J. Quantum Electron.*, vol. 27, n. 1, pp. 10–12, 1991.
- [8] D. Lenstra, B. H. Verbeek, and A. J. den Boef, "Coherence collapse in single-mode semiconductor lasers due to optical feedback," *IEEE J. Quantum Electron.*, vol. 21, n. 6, pp. 674–679, 1985.
- [9] M. Fujiwara, K. Kubota, and R. Lang, "Low frequency intensity fluctuations in laser diodes with external optical feedback," *Appl. Phys. Lett.*, vol. 38, n. 4, pp. 217–220, 1981.
- [10] J. Mork, B. Tromborg, and J. Mark, "Chaos in semiconductor lasers with optical feedback: Theory and experiment," *IEEE J. Quantum Electron.*, vol. 28, n. 1, pp. 93–108, 1992.
- [11] Ch. Risch and C. Vouard, "Self-pulsation in the output intensity and spectrum of GaAs-AlGaAs cw diode lasers coupled to a frequency-selective external optical cavity," *J. Appl. Phys.*, vol. 48, n. 5, pp. 2083–2085, 1977.
- [12] I. Fischer, G. H. M. Tartwijk, A. M. Levine, W. Elsasser, E. Gobel and D. Lenstra, "Fast pulsing and chaotic itinerancy with a drift in the coherence collapse of semiconductor lasers," *Phys. Rev. Lett.*, vol. 76, n. 2, pp. 220–223, 1996.
- [13] J. Mulet, C. R. Mirasso, "Numerical statistics of power dropouts based on the Lang-Kobayashi model," *Phys. Rev. E*, vol. 59, n. 5, pp. 5400–5405, 1999.
- [14] J. Mork, B. Tromborg, P.L. Christiansen, "Bistability and low-frequency fluctuations in semiconductor lasers with optical feedback: a theoretical analysis," *IEEE J. Quant. Electron.*, vol. 24, n. 2, pp. 123–133, 1988.
- [15] J. Sacher, W. Elsasser, E.O. Gobel, "Intermittency in the coherence collapse of a semiconductor laser with external feedback," *Phys. Rev. Lett.*, vol. 63, n. 20, pp. 2224–2227, 1989.
- [16] T. Sano, "Antimode dynamics and chaotic itinerancy in the coherence collapse of semiconductor lasers with optical feedback," *Phys. Rev. A*, vol. 50, pp. 2719–2726, 1994.
- [17] R. Lang and K. Kobayashi, "External optical feedback effects on semiconductor injection laser properties," *IEEE J. Quantum Electron.*, vol. 16, n. 3, pp. 347–355, 1980.
- [18] A. Hohl, H.J.C. van der Linden and R. Roy, "Determinism and stochasticity of power-dropout events in semiconductor lasers with optical feedback," *Opt. Lett.*, vol. 20, n. 23, pp. 2396–2398, 1995.
- [19] D.W. Sukow, J.R. Gardner, and D.J. Gauthier, "Statistics of power-dropout events in semiconductor lasers with time-delayed optical feedback," *Phys. Rev. A*, vol. 56, n. 5, pp. 3370–3373, 1997.
- [20] C. H. Henry, R.F. Kazarinov, "Instability of semiconductor lasers due to optical feedback from distant reflectors," *IEEE J. Quantum Electron.*, vol. 22, n. 2, pp. 294–301, 1986.
- [21] G. Vaschenko, M. Giudici, J. J. Rocca, C. S. Menoni, J. R. Tredicce, and S. Balle, "Temporal dynamics of semiconductor lasers with optical feedback," *Phys. Rev. Lett.*, vol. 81, n. 25, pp. 5536–5539, 1998.
- [22] C. Masoller and N. B. Abraham, "Polarization dynamics in vertical-cavity surface-emitting lasers with optical feedback through a quarter-wave plate," *Appl. Phys. Lett.*, vol. 74, n. 8, pp. 1078–1080, 1999.
- [23] M. C. Soriano, M. Yousefi, J. Danckaert, S. Barland, M. Romanelli, G. Giacomelli, and F. Marin, "Low-frequency fluctuations in vertical-cavity surface-emitting lasers with polarization selective feedback: experiment and theory," *IEEE J. Sel. Top. Quantum Electron.*, vol. 10, n. 5, pp. 998–1005, 2004.
- [24] R. Badii, N. Matuschek, T. Pliška, J. Troger, and B. Schmidt, "Dynamics of multimode diode lasers with strong, frequency-selective optical feedback," *Phys. Rev. E*, vol. 68, 036605, 2003.
- [25] H. Aoyama, S. Tomida, R. Shogenji, J. Ohtsubo, "Chaos dynamics in vertical-cavity surface-emitting semiconductor lasers with polarization-selected optical feedback," *Optics Communications*, vol. 284, n. 5, pp. 1405–1411, 2011.
- [26] T. Heil, I. Fischer, and W. Elsasser, "Coexistence of low-frequency fluctuations and stable emission on a single high-gain mode in semiconductor lasers with external optical feedback," *phys. Rev A*, vol. 58, n. 4, pp. 2672–2675, 1998.
- [27] M. W. Pan, B. P. Shi, and G. R. Gray, "Semiconductor laser dynamics subject to strong optical feedback," *Opt. Lett.*, vol. 22, n. 3, pp. 166–168, 1997.
- [28] M. Sorel, G. Giuliani, A. Sciré, R. Miglierina, J. P. R. Laybourn, and S. Donati, "Operating regimes of GaAs-AlGaAs semiconductor ring lasers: experiment and model," *IEEE J. Quantum Electron.* vol. 39, n. 10, pp. 1187–1195, 2003.
- [29] J. Javaloyes and S. Balle, "Emission directionality of semiconductor ring lasers: A traveling-wave description," *IEEE J. Quantum Electron.* vol. 45, n. 5, pp. 431–438, 2009.
- [30] M. T. Hill, H. Dorren, T. de Vries, X. Leijtens, J. den Besten, B. Smalbrugge, Y. Oei, H. Binsma, G. Khoe, and M. Smit, "A fast low-power optical memory based on coupled micro-ring lasers," *Nature*, vol. 432, n. 7014, pp. 206–209, 2004.
- [31] J. J. Liang, S. T. Lau, M. H. Leary, and J. M. Ballantyne, "Unidirectional operation of waveguide diode ring lasers," *Appl. Phys. Lett.*, vol. 70, no. 10, pp. 1192–1194, 1997.
- [32] A. Wang, Y. Wang, and H. He, "Enhancing the bandwidth of the optical chaotic signal generated by a semiconductor Laser with optical feedback," *IEEE Photon. Technol. Lett.*, vol. 20, n. 19, pp. 1633–1635, 2008.
- [33] M. Waldow, T. Plotzing, M. Gottheil, M. Forst, J. Bolten, T. Wahlbrink, and H. Kurz, "25 ps all-optical switching in oxygen implanted silicon-on-insulator microring resonator," *Opt. Express.*, vol. 16, n. 11, pp. 7693–7702, 2008.
- [34] A. Bahrapour, R. Fallah, A. A. Ganjovi, and A. Bahrapour, "Theoretical investigation of dielectric corona pre-ionization TEA nitrogen laser based on transmission line method," *Optics & Laser Technology*, vol. 39, n. 5, pp. 1014–1019, 2007.
- [35] S. J. Chang, Y. D. Zhou, Y. C. Lin, S. L. Wu, C. H. Chen, T. C. Wen, and L. W. Wu., "GaN-based MSM photodetectors prepared on patterned sapphire substrates," *IEEE Photon. Technol. Lett.*, vol. 20, n. 22 pp. 1866–1868, 2008.
- [36] T. Krauss, P. J. R. Laybourn, and J. Roberts, "CW operation of semiconductor ring lasers," *Electronics Lett.*, vol. 26, n. 25, pp. 2095–2097, 1990.

- [37] S. Beri, L. Gelens, M. Mestre, G. Van der Sande, G. Verschaffelt, A. Sciré, G. Mezosi, M. Sorel, and J. Danckaert, "Topological insight into the non-Arrhenius mode hopping of semiconductor ring lasers," *Phys. Rev. Lett.*, vol. 101, n. 9, 093903, 2008.
- [38] L. Gelens, S. Beri, G. Van der Sande, G. Mezosi, M. Sorel, J. Danckaert, and G. Verschaffelt, "Exploring multistability in semiconductor ring lasers: Theory and experiment," *Phys. Rev. Lett.*, vol. 102, n. 19, 193904, 2009.
- [39] S. Beri, L. Mashal, L. Gelens, G. Van der Sande, G. Mezosi, M. Sorel, J. Danckaert, and G. Verschaffelt, "Excitability in optical systems close to z2-symmetry," *Phys. Lett. A*, vol. 374, n. 5 pp.739-743, 2010.
- [40] W. Coomans, S. Beri, G. Van der Sande, L. Gelens, and J. Danckaert, "Optical injection in semiconductor ring lasers," *Phys. Rev. A*, vol. 81, n. 3, 033802, 2010.
- [41] R. M. Nguimdo, G. Verschaffelt, J. Danckaert, and G. Van der Sande, "Loss of time-delay signature in chaotic semiconductor ring lasers," *Opt. Lett.*, vol. 37, n. 13, pp. 2541–2543, 2012.
- [42] L. Mashal, G. Van der Sande, L. Gelens, J. Danckaert, and G. Verschaffelt, "Square-wave oscillations in semiconductor ring lasers with delayed optical feedback," *Opt. Express*, vol. 20, n. 20, pp. 22503–22516, 2012.
- [43] R. M. Nguimdo, G. Verschaffelt, J. Danckaert, X. Leijtens, J. Bolk, and G. Van der Sande, "Fast random bits generation based on a single chaotic semiconductor ring laser," *Opt. Express*, vol. 20, n. 27, pp. 28603–28613, 2012.
- [44] Y. Liu, P. Davis, and Y. Takiguchi, "Recovery process of low-frequency fluctuations in laser diodes with external optical feedback", *Phys. Rev. E*, vol. 60, n. 6, pp. 6595–6601, 1999.
- [45] D. Brunner, X. Porte, M. C. Soriano, and I. Fischer, "Real-time frequency dynamics and high-resolution spectra of a semiconductor laser with delayed feedback," *Sci. Rep.*, vol. 2, 732, 2012.
- [46] I. V. Ermakov, G. Van der Sande and J. Danckaert, "Semiconductor ring laser subject to delayed optical feedback: bifurcations and stability", *Commun. Nonlinear Sci. Numer. Simul.* vol. 17, n. 12, pp. 4767–4779, 2012.
- [47] L. Gelens, L. Mashal, S. Beri, W. Coomans, G. Van der Sande, J. Danckaert, and G. Verschaffelt, "Excitability in semiconductor microring lasers: Experimental and theoretical pulse characterization," *Phys. Rev. A*, vol. 82, 063841, 2010.
- [48] R. J. Jones, P. S. Spencer, J. Lawrence and D. M. Kane, "Influence of external cavity length on the coherence collapse regime in laser diodes subject to optical feedback", *IEE Proc. Optoelectron.*, vol. 148, n. 1, pp. 7–12, 2001.



Lilia Mashal was born in Algeria. She received the B.Sc. degree in physics in 1997, from the Yarmouk University, Irbid, Jordan and the M.Sc. degree in physics in 1999 from the University of Jordan, Amman, Jordan. She has been holding a lecturer position at the Hebron University, Hebron, Palestine, since 2009. She is currently working toward a Ph.D. degree in applied sciences at Applied Physics Research Group (APHY), Vrije Universiteit Brussel, Brussels, Belgium. Her research focuses on the experimental and numerical study of semiconductor

ring lasers.



Romain Modeste Nguimdo was born in Fongo-Tongo, Cameroon, on March 15, 1981. He received the M.Sc. degree in theoretical physics from the University of Dschang (Cameroon), and the University of Yaoundé I, (Cameroon) in 2006, and the M.Sc. degree in theoretical physics and the Ph.D. degree, both from the Instituto de Física Interdisciplinar y Sistemas Complejos (CSIC-UIB), Palma de Mallorca, Spain, in 2008 and 2011, respectively. He is currently a postdoc fellow at Applied Physics Research Group, Vrije Universiteit Brussel, Brussels,

Belgium. His current research interests include nonlinear dynamics, optical chaos cryptography, and ultra-pure microwaves, random bit generation and reservoir computing.



Guy Van der Sande was born in Mechelen, Belgium, in 1978. He received the Graduate degree in electrotechnical engineering with a major in photonics from the Vrije Universiteit Brussel (VUB), Brussels, Belgium, in 2001. He received the title of Doctor in the applied sciences from the Department of Applied Physics and Photonics, VUB, in 2005. His Ph.D. program was focused on theoretical modeling of vertical-cavity surface-emitting lasers and nonlinear photonic crystals. He spent a year at the Department of Optique Nonlinéaire Théorique, Université Libre de Bruxelles. In 2006, he returned to the Department of Applied Physics and Photonics, VUB, as a Post-Doctoral Research Fellow of the Flemish Fund for Scientific Research. In 2007, he was a Visiting Scientist at the Institute for Cross-Disciplinary Physics and Complex Systems, Palma de Mallorca, Spain. Since 2013, he is a Research Professor at the Vrije Universiteit Brussel. His current research interests include nonlinear dynamics of delay-coupled semiconductor lasers, semiconductor ring lasers and bio-inspired information processing.



Miguel Cornelles Soriano was born in Benicarlo, Spain, in 1979. He is member of the IEEE Photonics Society. He received the Telecommunications Engineering degree from the Universitat Politècnica de Catalunya, Barcelona, Spain, in 2002 and the Ph.D. degree in applied sciences from the Vrije Universiteit Brussel, Brussels, Belgium, in 2006. He has been holding an assistant professor position at the Instituto de Física Interdisciplinar y Sistemas Complejos, Palma de Mallorca, Spain, since January 2011, where he previously held a 'Juan de la Cierva'

scientific contract. His main research interests include the experimental and theoretical study of semiconductor lasers subject to delayed optical feedback and the synchronization properties of delay-coupled semiconductor lasers in the chaotic regime. Additional research lines cover topics such as information processing based on reservoir computing and nonlinear dynamics.



Jan Danckaert was born in Antwerp (Belgium) in 1964, and graduated in Physics at the University of Antwerp in 1985. He then joined the Department of Applied Physics and Photonics (TONA) of the Vrije Universiteit Brussel (VUB, Brussels, Belgium) as a teaching assistant. In 1992, he obtained a PhD on the subject of nonlinear optics, studying the response of nonlinear optical resonators for all optical information processing. After a stay abroad at INPG in Grenoble, France (1993), he returned to the same department of the VUB. In 2001 and

2002 he was a visiting scientist at IFISC (Institute for Cross-Disciplinary Physics and Complex Systems), Palma de Mallorca, Spain. As from 2005 on he is a full-time professor at the VUB, teaching introductory physics for both science and (bio-) engineering students, and courses in photonics at Master level. His current research interests go towards semiconductor laser dynamics in particular and nonlinear dynamics in general. Currently, he is head of the Applied Physics (APHY) research group at the VUB.



Guy Verschaffelt was born in Belgium in 1973. He received the M.E. degree in photonics and the Ph.D. degree from the Vrije Universiteit Brussel (VUB), Brussels, Belgium in 1996 and 2000, respectively. Presently, he is a postdoctoral researcher with VUB. His research interests include polarization and noise properties of vertical-cavity surface-emitting lasers, emission properties of broad-area high power semiconductor lasers and the dynamics of semiconductor ring lasers.